Expression of doubly labeled *Saccharomyces cerevisiae iso*-1 ferricytochrome *c* and ^{1}H, ^{13}C and ^{15}N chemical shift assignments by multidimensional NMR

Christina M. Szabo[1], Lori K. Sanders, H. Carl Le, Ellen Y.T. Chien[2], Eric Oldfield*

Department of Chemistry, University of Illinois at Urbana-Champaign, 600 South Mathews Avenue, Urbana, IL 61801, USA

Abstract We have expressed [U-^{13}C,^{15}N]-labeled *Saccharomyces cerevisiae iso*-1 cytochrome *c* C102T;K72A in *Escherichia coli* with a yield of 11 mg/l of growth medium. Nuclear magnetic resonance (NMR) studies were conducted on the Fe^{3+} form of the protein. We report herein chemical shift assignments for amide ^{1}H and ^{15}N, ^{13}C°, ^{13}C$^\alpha$, ^{13}C$^\beta$, ^{1}H$^\alpha$ and ^{1}H$^\beta$ resonances based upon a series of three-dimensional NMR experiments: HNCA, HN(CO)CA, HNCO, HN(CA)CO, HNCACB, HCA(CO)N, HCCH-TOCSY and HBHA(CBCA)NH. An investigation of the chemical shifts of the threonine residues was also made by using density functional theory in order to help solve discrepancies between ^{15}N chemical shift assignments reported in this study and those reported previously. © 2000 Federation of European Biochemical Societies. Published by Elsevier Science B.V. All rights reserved.

Key words: Cytochrome *c*; Nuclear magnetic resonance; Chemical shift assignment; *Saccharomyces cerevisiae*

1. Introduction

Low expression levels of yeast *iso*-1 cytochrome *c* (cyt *c*) have precluded the ready isotopic incorporation of ^{13}C labels for nuclear magnetic resonance (NMR) spectroscopy. A limited number of ^{13}C assignments have previously been reported for ferrocytochrome *c* using measurements made on concentrated samples at natural abundance [1], but previous structural studies of ferricytochrome *c* have relied on ^{1}H NMR data (assignments [2], NOEs and pseudocontact shifts [3]), and despite low yields, ^{15}N-labeled ferricytochrome *c* has been prepared for hydrogen exchange and dynamics measurements by using large-scale fermentation [4–6]. However, the construction by Pollock et al. [7] of a plasmid which encodes the coexpression of cyt *c* heme lyase has recently permitted the expression of the yeast protein in *Escherichia coli*, with much higher yields. The protein expressed in *E. coli* lacks the post-translational modification (trimethylation) of K72 and, though spectroscopically equivalent at pH 7, has a slightly lower pK_a for the alkaline conformational transition than that obtained from yeast. The C102T;K72A mutant, which

is more stable at mildly alkaline pH, has been engineered by Mauk and coworkers [7] and is the subject of this investigation. While this work was in progress, Pielak et al. have also made use of a similar expression system to express ^{15}N-labeled ferricytochrome *c* C102T [8], to study ^{1}H and ^{15}N hyperfine shifts [9].

The desire to incorporate additional spectroscopic restraints into a solution structure determination prompted us to express [U-^{13}C,^{15}N]-labeled yeast *iso*-1 cyt *c* in *E. coli* in order to provide a data base of dipolar splittings [10], ^{1}H, ^{13}C and ^{15}N NMR shifts [11] and shift anisotropies [12], to be used in structure refinement, using in some cases quantum chemical techniques. It has been shown previously that quantum chemistry can be used to predict ^{1}H, ^{13}C, ^{15}N and ^{19}F chemical shifts in proteins [13], and that ^{15}N shifts are dependent primarily on local backbone dihedral angles, ϕ_i and ψ_{i-1} [14]. Here, in addition to providing most backbone ^{1}H, ^{13}C and ^{15}N shifts, together with those of C^β, we demonstrate that quantum chemical (density functional theory (DFT)) calculations can be used to validate spectroscopic assignments, which can be of particular utility when differences between assignments from different groups are apparent.

2. Materials and methods

2.1. Protein expression and purification

The plasmid for *Saccharomyces cerevisiae iso*-1 cyt *c* K72A;C102T, pBTR2, was the kind gift of Professor A.G. Mauk. Freshly transformed *E. coli* cells (Epicurian coli BL21(DE3) Gold competent cells, Stratagene, La Jolla, CA, USA) were spread on an LB-ampicillin plate and incubated at 37°C overnight. A single colony from the plate was used to inoculate 5 ml of LB [15]. After overnight incubation at 37°C and 220 rpm, 50 μl of culture was used to inoculate 50 ml of growth medium, which was similarly incubated and shaken until mid-log phase (5–6 h). This culture was then used as a 1% inoculation for 600 ml of medium, which was first incubated at 37°C and 200 rpm for 18 h and then at 150 rpm for 4 h, prior to harvesting the cells. All growth media were supplemented with 0.2 mg/ml ampicillin (Sigma, St. Louis, MO, USA).

The purification scheme was loosely based on that described by Mauk and coworkers [7]. The cell paste was first flash frozen in dry ice. Then, lysis was achieved by stirring the cell paste in three times its volume of Bacterial Protein Extraction Reagent (Pierce, Chemical Co., Rockford, IL, USA) containing 1 mM EDTA, 1 mM PMSF, 40 U/ml DNase, 4 U/ml RNase and 3 mg/ml lysozyme, at room temperature. Subsequent purification steps were conducted at 4°C. After ultracentrifugation, the cell pellet was redissolved in lysis buffer and centrifuged. The supernatants from each lysis were combined and subjected to fractionation with a 55% saturated $(NH_4)_2SO_4$ solution. The protein solution was centrifuged and the supernatant dialyzed against 46 mM NaP_i, pH 6.8. The resulting dialysate was then loaded onto a CM52 cation exchange column (Whatman International Ltd., Maidstone, UK), which was equilibrated with the same buffer. The

*Corresponding author. Fax: (1)-217-244 0997.
E-mail: eo@chad.scs.uiuc.edu

protein was eluted with equilibration buffer containing 250 mM NaCl. Fractions which were >80% pure, as determined by UV-vis absorption [16] and SDS–polyacrylamide gel electrophoresis, were combined and exchanged with 46 mM NaP$_i$, pH 6.8. The protein solution was then loaded onto a CM52 column that had been equilibrated with 20 mM NaP$_i$, pH 7.0. The protein was eluted with equilibration buffer with a linear [NaCl] gradient, from 0 to 300 mM. Those fractions that were >95% pure were combined, exchanged with 50 mM NaP$_i$, pH 7.0, and concentrated using a YM-3 (Amicon, Beverly, MA, USA) membrane in an Amicon stirred cell, followed by 3000 MWCO Centricon and Microcon centrifugal concentrators (Millipore Corporation, Bedford, MA, USA).

^{13}C,^{15}N-labeled protein was expressed by growing cells in an isotopically labeled growth medium at the 50 ml and 0.6 l scales, using a mixture of a modified M9 minimal medium [17] and Celtone-CN (Martek Biosciences Corporation, Columbia, MD, USA) in a 6:4 ratio. Electrospray mass spectrometry data indicated essentially complete isotopic labeling (experimental mass = 13 296 Da, theoretical mass = 13 334 Da). (^{15}NH$_4$)$_2$SO$_4$, ^{15}NH$_4$Cl and [U-^{13}C]glucose were from Cambridge Isotope Laboratories (Andover, MA, USA).

2.2. NMR spectroscopy

Purified protein was oxidized with a slight excess of K$_3$Fe(CN)$_6$, which was then removed by exchanging with 50 mM NaP$_i$, pH 7.0. D$_2$O (Aldrich, Milwaukee, WI, USA) was added to a final concentration of 10% by volume. The first sample was 0.5 mM in cyt *c*, and was used for the majority of the experiments; a second sample was prepared at 1.5 mM, and yielded indistinguishable NMR chemical shifts.

A suite of sensitivity-enhanced three-dimensional (3D) triple resonance experiments were performed by using a Varian (Palo Alto, CA, USA) Inova 17.6 T NMR spectrometer. A Varian 5 mm ^{1}H{^{13}C,^{15}N} pulsed field gradient probe was utilized, and the temperature was regulated to 38 ± 1°C. The following experiments were used for sequential resonance assignments: HNCO [18], HN(CA)CO [19], HNCA [20], HN(CO)CA [19] and HNCACB [21]. Spectral parameters were as follows: a recycle delay of 0.6 s was used in each experiment. Typical spectral widths were 13 502, 2280, 2264, 6855 and 11 053 Hz for the ^{1}H, ^{15}N, ^{13}C°, ^{13}C$^\alpha$ and ^{13}C$^\alpha$-^{13}C$^\beta$ regions, and 90° pulse widths were 7 μs for ^{1}H, 12.4 μs for ^{13}C and 35 μs for ^{15}N. Other experimental conditions were as follows: the HNCO experiment was acquired with 2048×52×64 data points in each of the ^{1}H, ^{13}C and ^{15}N dimensions, respectively, with 32 scans per FID, yielding a total acquisition time of 92 h; HN(CA)CO: 2048×89×32 (^{1}H, ^{13}C, ^{15}N) data points, 32 scans (110 h); HNCA: 2048×86×40 (^{1}H, ^{13}C, ^{15}N) data points, 32 scans (92 h); HN(CO)CA: 2048×60×32 (^{1}H, ^{13}C, ^{15}N) data points, 16 scans (26 h); HNCACB: 2048×50×32 (^{1}H, ^{13}C, ^{15}N) data points, 32 scans (43 h). Proton chemical shifts were referenced to external DSS (dimethylsilapentane-5-sulfonic acid, Thompson Packard, Inc., Little Falls, NJ, USA), and the ^{13}C and ^{15}N chemical shifts were indirectly referenced using the 'consensus' Ξ ratios, as described by Wishart et al. [22]. The δ-scale, in which high frequency, low-field, paramagnetic or deshielded values are positive, was used.

Data were processed using Felix 98.0 (Molecular Simulations, Inc., San Diego, CA, USA) on a Silicon Graphics (SGI, Mountain View, CA, USA) Origin 200 workstation. Suppression of the residual water signal was achieved by post-acquisition time-domain convolution with a sinebell function. The downfield half of the directly detected ^{1}H dimension (amide region) was extracted for further processing. Linear prediction was used to extend the number of data points in the indirectly detected ^{13}C and ^{15}N dimensions by a factor of two, then zero-filling was used to yield a 1024×256×128 point matrix in the ^{1}H, ^{13}C and ^{15}N dimensions, respectively. A 90° phase-shifted (sinebell)^2 apodization function was applied over all acquired and linear predicted data points. A two-dimensional (2D) ^{15}N-^{1}H HSQC spectrum [23] with WET [24] solvent suppression was acquired with ^{1}H and ^{15}N spectral widths of 16 502 Hz and 4561 Hz, respectively. The data consisted of 128 points in t_1 and 2048 points in t_2, and 16 scans per FID. Processing conditions were as described above. An expansion of the HSQC spectrum is shown in Fig. 1. A 3D HCA(CO)N experiment [25] was performed in 57 h (sweep width (Hz), number of increments: 7502, 1152 (^{1}H); 4605, 30 (^{13}C); 2824, 72 (^{15}N)) with 32 scans per FID. Processing parameters were identical to those described above, except that the full ^{1}H spectrum was used, and zero-filling was applied such that the resulting matrix contained 1024×128×256 data points in the ^{1}H, ^{13}C and ^{15}N dimensions, re-

spectively. A 3D HCCH-TOCSY [26] data set was acquired in 81 h (2048×104×60 data points with 13502, 13502 and 12941 Hz spectral windows in the observed ^{1}H, indirectly detected ^{1}H, and ^{13}C dimensions, respectively). A 3D HBHA(CBCA)NH [27] data set was acquired in 63 h (2048×70×32 data points with 13502, 10499 and 2500 Hz spectral windows in the observed ^{1}H, indirectly detected ^{1}H, and ^{15}N dimensions).

2.3. Computational aspects

DFT calculations of threonine ^{15}N chemical shieldings were performed by using the gauge-including atomic orbitals approach [28,29] in the Gaussian 98 [30] program (Gaussian, Inc., Pittsburgh, PA, USA). An *N*-formyl-L-alanyl-threonine amide model fragment was energy-minimized using an AMBER forcefield [31,32] in the Discover module of Insight II® (Molecular Simulations, Inc., San Diego, CA, USA). Following minimization, the $\phi_{(i-1)}$, $\psi_{(i-1)}$, ϕ_i and ψ_i torsion angles were set to the X-ray values, while the χ_1 angle was set to the staggered minimum energy conformer ($\chi_1 = 60$, -60 or 180) nearest to the X-ray χ_1 value [33]. A locally dense [34] basis set approach was employed using a 6-311++G(2d,2p)/6-31G scheme, with the larger basis placed on the atoms in bold depicted in the following structure:
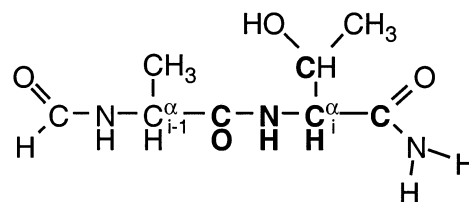
DFT calculations employed the Becke 1988 exchange functional [35] and the Perdew/Wang 1991 correlation functional [36] (BPW91). Calculations were carried out by using Silicon Graphics Origin 200 computers in this laboratory as well as on Silicon Graphics Origin 2000 and HP-Convex Exemplar SP-2000 (Hewlett Packard Company, Palo Alto, CA, USA) computers, located in the National Center for Supercomputing Applications in Urbana, IL, USA. The experimental threonine torsion angles employed in these calculations were obtained from the Research Collaboratory for Structural Bioinformatics Protein Data Bank [37], for the following proteins: bovine pancreatic trypsin inhibitor (5pti) [38], ubiquitin (1ubq) [39] and cyt *c* (2ycc) [40].

3. Results and discussion

Previous expression methods made use of the yeast strain C93, which produced yeast cyt *c* C102T in yields of 0.4 mg per liter of growth medium [4]. The expression system for this protein in *E. coli* developed by Mauk and coworkers [7] has recently been used for the production of ^{15}N-labeled protein in much higher yields (8 mg/l) [8], which makes the preparation of doubly labeled proteins feasible. We have used a similar system in *E. coli* to express doubly labeled cyt *c* C102T;K72A. Using our mixture of modified M9 minimal medium and Celtone, we obtained 14 mg/l of [U-^{15}N]-labeled and 11 mg/l of [U-^{13}C,^{15}N]-labeled cyt *c*.

The combination of the HNCA, HN(CO)CA, HNCACB, HNCO and HN(CA)CO experiments allowed for the sequential assignment of backbone ^{1}H and ^{15}N, ^{13}C°, ^{13}C$^\alpha$ and ^{13}C$^\beta$ chemical shifts. Previous ^{1}H and ^{15}N assignments [2,5], together with a comparison of the primary sequence with ^{13}C$^\alpha$ and ^{13}C$^\beta$ shift patterns, facilitated initial residue-specific chemical shift assignments, while the HCA(CO)N, HCCH-TOCSY and HBHA(CBCA)NH experiments permitted the elucidation of ^{1}H$^\alpha$ and ^{1}H$^\beta$ chemical shifts. Fig. 2 shows a representative HNCACB strip plot, which illustrates the sequential connectivities between residues 31 and 44. Table 1 lists the specific ^{1}H, ^{15}N and ^{13}C chemical shift assignments for cyt *c*. The first two residues of the sequence, together with

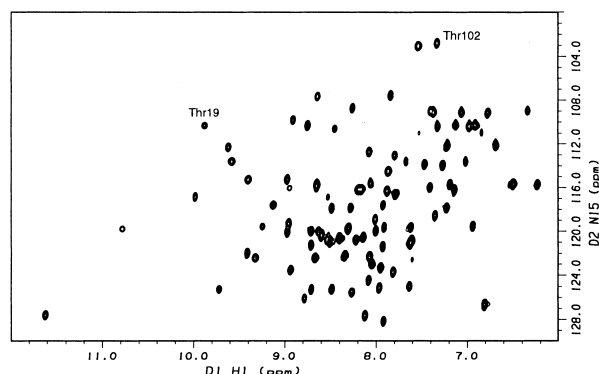Fig. 1. An expansion of the 2D ^{15}N-^{1}H HSQC spectrum at 38°C. See text for details.

Gly83 and Gly84 (except for G84:H$^\alpha$), remain to be assigned, despite the efforts of several groups [2,3,5]. The double-Gly is within a region near the connection between loop D and the terminal helix C, for which we currently lack assignments for reasons that are at this time unknown.

The amide ^{1}H and ^{15}N chemical shifts presented here are in general agreement with those reported by Fetrow and Baxter [5], with the exception of the ^{15}N shifts corresponding to residues: 19, 21, 23, 56, 72, 73, 75, 79, 80, 81 and 102, where there are typically shift differences of ~2 parts per million (ppm). However, in the cases of Thr19 and Thr102, the shift differences are 18.5 and 24.0 ppm, respectively. Of the 11 variant shifts, the more recent assignments by Pielak et al. [8] show amide ^{15}N chemical shifts for Thr19, Asn56, Lys79, Ala81 and Thr102 which are in very close agreement with the results we have obtained. One possibility for the discrepancies is that the peak at 102.6 ppm, which we assign to ^{15}N^H of Thr102, may have been folded in the ^{15}N NOESY-HSQC spectra of the initial study, based on the reported spectral width in the ^{15}N dimension (1250 Hz at 11.7 T, centered at 118.5 ppm; 106.2–130.8 ppm). If this peak was in fact folded, it would place the actual ^{15}N resonance at 101.9 ppm, which is only 0.7 ppm upfield of the assignment presented here and 0.2 ppm upfield of that shown in the spectrum of Pielak et al. [8]. We verified that the peaks were not folded in our spectra by acquiring 2D ^{15}N-^{1}H planes in the HNCACB experiment with a larger spectral width (up to 100 ppm) and with different ^{15}N carrier frequencies (115.0 and 106.0 ppm). The discrepancy between the ^{15}N^H assignment of Thr19 does not seem to be

due to folding. However, there does appear to be an unassigned crosspeak in the original ^{15}N HSQC spectrum at ~10 ppm (δ^1H) and 110 ppm (δ^{15}N) which may correspond to Thr19 [4]. Such an assignment would then be in agreement with the assignment by Pielak et al. [8] and that obtained here. The crosspeaks corresponding to Thr19 and Thr102 are labeled in the 2D ^{15}N-^{1}H HSQC spectrum shown in Fig. 1. The additional mutation at residue 72 (K72A) in the protein we have investigated may account for the small differences in chemical shift seen for residues 72, 73 and 75 from those reported previously, due to near-neighbor effects.

In previous work [13,33,41,42], we have had some success in predicting chemical shifts in proteins and peptides using quantum chemical techniques. We therefore extended these methods here by using DFT calculations to investigate the >18 ppm discrepancies in our backbone amide ^{15}N shifts of Thr19 and Thr102 with those reported previously [5], basically to test the idea that DFT calculations may be of use in confirming, or clarifying, spectroscopic assignments. For this we chose two proteins, BPTI and ubiquitin, which are well-characterized by both NMR and X-ray crystallography, to serve as a small data base to check the accuracy of ^{15}N NMR shielding calculations for threonine residues. The theoretical chemical shielding results from DFT calculations for these two proteins, and for cyt c, were then compared with the experimental NMR chemical shift results for BPTI [43], ubiquitin [44] and the cyt c results from this work. We found a good correlation between the experimental shifts and theoretical shieldings for the two reference proteins (BPTI, ubiquitin) with a slope of −0.75 and an R^2 of 0.86, as shown in Fig. 3 (○). For BPTI and ubiquitin, the threonine χ_1 torsion angles determined via X-ray [38,39] agree with the values found in the well-defined, high resolution NMR structures [45,46] with the exception of ubiquitin Thr14. For the Thr14 calculation, the χ_1 angle was therefore rotated from +60 (X-ray) to −60 (solution). This modification removed Thr14 as an outlier and improved the theory vs. experiment slope and correlation. We also show in Fig. 3 the experimental shifts/computed shieldings for the eight threonines in cyt c, based on the assignments presented in Table 1 and the crystallographic coordinates for yeast iso-1 cyt c. Seven of the eight cyt c points (▲) fall very near the BPTI/ubiquitin correlation line, while the datum for Thr8 falls off the line (predicted shielding = 137.9 ppm). However, if the χ_1 torsion angle of Thr8 is likewise changed from +60 to −60, this point now falls very close to the correlation line (×, predicted shielding = 126.2 ppm), suggestive of a crys-
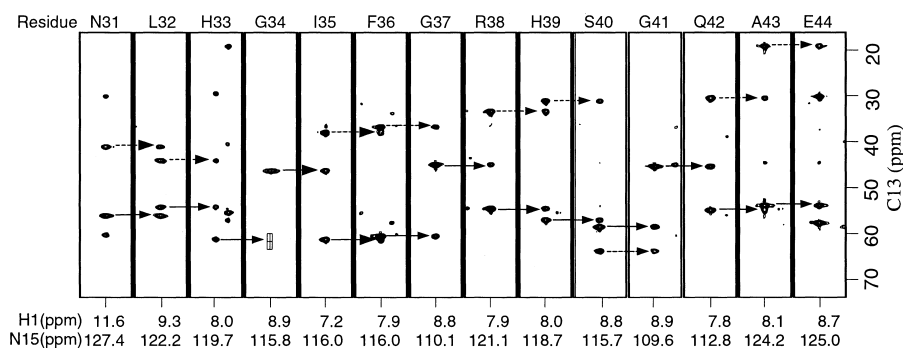

Fig. 2. Strip plot of the 3D HNCACB experiment showing 2D ^{1}H-^{13}C planes at the given ^{15}N frequency, with arrows showing the i to i+1 connectivities. The solid arrows show connectivities between ^{13}C$^\alpha$ resonances, and the dashed arrows correspond to those between ^{13}C$^\beta$ resonances.

Table 1
Chemical shift assignments of yeast *iso*-1 cyt *c* C102T;K72A, pH 7.0, 311 K in 50 mM NaP$_i$, with external DSS as a ^{1}H shift reference (0.0 ppm)

Residue	Amide ^{1}H	Amide ^{15}N	^{13}C°	^{13}C$^\alpha$	^{13}C$^\beta$	^{1}H$^\alpha$, ^{1}H$^{\alpha 2}$ [a]	^{1}H$^{\beta 1}$, ^{1}H$^{\beta 2}$ [a]
Glu−4			175.6	56.2	30.8	4.31	2.0
Phe−3	8.53	124.0	174.5	58.6	39.6	4.34	2.87, 2.63
Lys−2	6.65	127.0	173.3	54.7	34.3	3.82	1.28, 1.42
Ala−1	7.61	122.3	178.2	53.3	18.7	3.64	1.24
Gly1	8.02	110.2	173.0	43.9		4.31, 3.42	
Ser2	9.37	119.6	175.5	55.6	63.1	4.74	3.82, 3.61
Lys4			179.3	59.7		4.01	
Lys5	7.68	119.9	180.5	58.4	32.1	4.08	1.71
Gly6	8.65	107.4	174.2	47.1		4.00, 3.28	
Ala7	7.97	124.9	180.5	54.8	18.5	2.40	1.20
Thr8	7.20	115.5	177.2	66.5	68.4	3.88	4.18
Leu9	7.82	123.6	177.8	58.1	42.8	3.81	1.82, 0.84
Phe10	8.61	120.1	178.6	62.9	40.0	3.49	2.74, 2.96
Lys11	8.40	120.5	177.7	60.2	32.7	4.30	2.13
Thr12	7.84	107.3	176.7	64.0	70.4	4.36	4.22
Arg13	8.20	116.1	176.8	55.5	31.3	4.6	1.43, 1.07
Cys14	7.87	114.3	177.7	55.3	37.4	4.72	2.71, 1.4
Leu15	7.95	123.2	177.3	58.0	44.0	5.91	2.47, 2.08
Gln16	9.88	117.6	177.6	59.4	28.8	4.72	2.63, 2.43
Cys17	9.58	113.4	176.1	58.1	37.2	6.03	2.47
His18	10.78	119.5	175.8	40.2		8.6	
Thr19	9.88	110.1	176.4	60.9	72.7	6.14	5.37
Val20	8.46	110.5	174.3	62.4	34.2	4.81	2.15
Glu21	9.24	119.4	178.1	57.6	30.2	4.46	2.19
Lys22	8.79	125.9	178.1	58.7	31.5	3.38	1.5, 0.7
Gly23	9.37	117.9	174.9	45.5		4.06, 3.63	
Gly24	8.26	108.6	170.8	44.5		4.37, 3.65	
Pro25			179.4	62.6	32.1		
His26	8.64	121.1	175.8	56.2	30.8	5.01	3.08, 2.75
Lys27	8.27	125.4	176.0	55.9	32.6	4.69	2.4, 2.1
Val28	7.41	121.5	176.2	65.8	32.9	3.12	1.3
Gly29	7.54	102.9	168.8	38.3		−2.84, −0.10	
Pro30			178.0	60.5	29.9	3.81	1.4, −0.1
Asn31	11.63	127.4	176.8	56.3	41.0	5.68	2.87, 2.49
Leu32	9.32	122.3	175.4	54.4	44.1	4.70	2.2, 1.9
His33	8.00	119.8	178.3	61.4	29.2	4.00	
Gly34	8.95	115.8	175.2	46.4		3.78, 3.76	
Ile35	7.14	116.1	174.1	61.5	37.9	3.66	1.64
Phe36	7.88	116.1	176.9	60.7	36.6	4.08	2.89
Gly37	8.75	110.1	173.1	45.1		4.27, 3.65	
Arg38	7.93	121.1	174.7	54.7	33.3	4.47	1.98, 1.8
His39	8.01	118.7	177.0	57.2	30.9	5.15	2.92, 2.75
Ser40	8.66	115.8	175.2	58.7	63.8	4.52	4.16, 3.61
Gly41	8.91	109.5	174.6	45.5		3.10, 1.12	
Gln42	7.80	112.9	176.4	55.1	30.3	4.47	2.42, 1.69
Ala43	8.09	124.2	178.2	54.1	18.7	4.34	1.42
Glu44	8.71	125.1	178.7	57.9	29.9	4.12	2.07
Gly45			172.8	45.9		4.27, 3.70	
Tyr46	6.94	119.3	173.4	57.2	39.0	3.68	1.64, 0.63
Ser47	6.39	122.1	171.4	55.9	61.5	4.08	3.17, 3.00
Tyr48	7.64	124.8	178.9	58.5	41.6	4.16	3.29, 2.50
Thr49	9.62	112.0	176.0	62.6	71.1	4.17	4.60
Asp50	8.54	120.6	178.7	57.3	40.4	4.35	2.63, 2.56
Ala51	7.92	119.5	179.6	55.6	18.9	4.09	1.59
Asn52	8.28	117.7	178.3	56.1	40.4	4.67	3.14, 2.91
Ile53	7.61	120.6	178.6	65.3	39.3	3.65	1.86
Lys54	8.96	119.2	177.8	58.1	32.2	3.94	1.86
Lys55	7.36	118.3	176.8	57.3	31.5	4.07	2.01
Asn56	7.24	112.1	174.1	54.2	37.7	4.36	3.02, 2.3
Val57	7.27	113.9	173.7	59.6	33.6	4.12	1.36
Leu58	8.12	127.4	176.8	53.8	41.3	3.81	1.49, 0.86
Trp59	7.93	128.0	176.2	58.2	29.9	4.91	3.58, 2.38
Asp60	9.72	125.1	175.0	52.5	42.9	4.82	3.0, 2.8
Glu61	9.99	116.7	177.4	61.6	29.0	3.41	1.35
Asn62	8.16	116.1	178.3	56.3	38.8	4.45	2.88
Asn63	9.42	121.7	179.4	56.2	36.7	4.57	3.2, 2.9
Met64	8.71	121.1	177.9	57.6	30.6	4.35	2.2, 1.75
Ser65	7.47	113.6	177.4	61.7	62.9	3.57	4.14, 3.86
Glu66	7.63	121.0	179.8	60.3	29.5	3.87	2.08, 1.97
Tyr67	8.35	122.0	177.0	60.9	39.3	4.15	3.29, 3.04
Leu68	8.08	112.6	177.4	55.7	41.1	2.96	1.10, 0.15

Table 1 (*continued*)

Residue	Amide ^{1}H	Amide ^{15}N	^{13}C°	^{13}C$^\alpha$	^{13}C$^\beta$	^{1}H$^\alpha$, ^{1}H$^{\alpha2}$ [a]	^{1}H$^{\beta1}$, ^{1}H$^{\beta2}$ [a]
Thr69	7.41	115.8	174.6	66.7	68.6	3.82	4.17
Asn70	6.78	108.9	173.7	52.7	37.7	4.89	3.21, 3.10
Pro71			178.0	68.0	33.8	5.56	
Ala72	9.13	117.4	179.7	54.8	19.0	5.10	2.11
Lys73	7.79	116.4	177.6	57.9	33.8	4.45	2.11, 2.03
Tyr74	8.22	120.6	176.5	62.2	40.9	4.70	4.09, 3.88
Ile75	9.40	115.1	171.0	59.9	38.4	4.72	3.32
Pro76			179.1	64.5	31.5	5.10	2.6, 2.1
Gly77	9.36	112.0	176.2	45.0		3.90, 4.6	
Thr78	8.97	115.1	173.4	62.0	70.2	5.07	5.70
Lys79	8.05	122.9	175.0	55.3	32.0	4.79	1.70, 1.36
Met80	8.67	122.3	173.9	67.3			
Ala81	8.09	139.0	175.0[b]	51.9	16.9	5.07	1.27
Phe82	8.56	122.6	175.4[b]	58.0	42.5	4.7	
Glu88			177.5	60.2	29.5	3.42	1.98
Lys89	8.53	116.7	177.7	59.6	32.4	3.82	1.8, 1.56
Asp90	6.24	115.5	177.9	56.9	40.2	4.04	2.63, 2.21
Asn91	7.23	117.7	177.5	61.2	30.2	3.28	1.85, 1.3
Asn92	8.49	117.7	179.6	56.1	37.0	4.4	2.84, 2.6
Asp93	8.49	125.1	177.6	58.9	40.0	4.05	2.5
Leu94	8.14	120.4	178.8	58.7	41.2	3.82	1.38, 1.30
Ile95	8.71	119.8	176.2	66.2	37.2	3.07	1.76
Thr96	7.93	117.4	176.8	68.3		3.70	4.2
Tyr97	7.62	119.5	176.1	61.5	37.9	4.05	3.52, 2.89
Leu98	8.97	119.8	179.1	57.5	42.8	3.24	1.45, 1.26
Lys99	8.51	120.8	177.0	59.1	31.3	3.36	1.43, 1.18
Lys100	6.50	115.5	178.7	57.3	32.4	4.15	1.8
Ala101	8.30	119.5	178.7	54.1	18.9	4.02	0.67
Thr102	7.34	102.6	173.2	61.4	70.0	4.63	4.82
Glu103	6.81	126.4	181.5	58.5	30.8	4.06	2.32, 2.00

[a]Not stereospecifically assigned.
[b]Tentative assignments.

tal solution structural difference, as deduced previously for five of the seven valine residues in calmodulin [33]. These conformational changes are also supported by the ^{13}C$^\alpha$ chemical shielding values, which improve for both ubiquitin Thr14 and cyt *c* Thr8 upon χ_1 rotation, resulting in an $R^2 = 0.71$ versus $R^2 = 0.63$, further supporting these small conformational differences between the X-ray and solution NMR structures.

The root mean square deviation for the full set of 18 calculated points is 2.4 ppm (slope = −0.73, $R^2 = 0.78$, Fig. 3). In sharp contrast, the use of the earlier assignments for Thr19 and Thr102 clearly leads to pronounced deviations for these two residues (of 14.7 ppm and 15.4 ppm, respectively) from the correlation line. The slope and intercept of the BPTI/ubiquitin correlation line can also be used to convert the predicted absolute shieldings (the shielding from the bare nitrogen atom) computed via DFT to chemical shifts, in which case we find predicted shifts of 109.0 ppm and 105.0 ppm for Thr19 and Thr102, in very good accord with the 110.5 and 102.6 ppm values seen experimentally. This is consistent with both our assignments and those reached independently by Pielak et al. [8].

In conclusion, the results we have reported above are of interest since they show that a yeast *iso*-1 type cyt *c* can be readily double-labeled for 3D NMR investigations, and that quantum chemical calculations (DFT) can be used to help clarify, at least in some cases, questions about spectroscopic assignments which might otherwise be more costly and time-consuming to obtain.
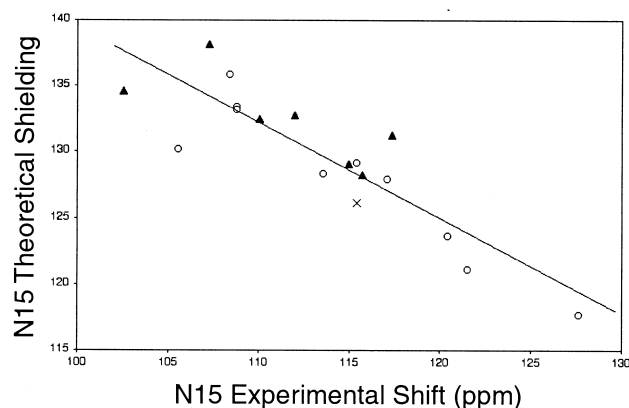

Fig. 3. Graph showing correlation between experimental threonine ^{15}N chemical shifts and DFT theoretical shieldings for BPTI and ubiquitin (○) and cyt *c* (▲, ×): slope = −0.73, $R^2 = 0.78$. See text for details.

References

[1] Sukits, S.F. and Satterlee, J.D. (1997) J. Prot. Chem. 16, 775–786.

[2] Gao, Y., Boyd, J., Williams, R.J.P. and Pielak, G.J. (1990) Biochemistry 29, 6994–7003.

[3] Banci, L., Bertini, I., Bren, K.L., Gray, H.B., Sompornpisut, P. and Turano, P. (1997) Biochemistry 36, 8992–9001.

[4] Baxter, S.M., Boose, T.L. and Fetrow, J.S. (1997) J. Am. Chem. Soc. 119, 9899.

[5] Fetrow, J.S. and Baxter, S.M. (1999) Biochemistry 38, 4480–4492.

[6] Baxter, S.M. and Fetrow, J.S. (1999) Biochemistry 38, 4493–4503.

[7] Pollock, W.B.R., Rosell, F.I., Twitchett, M.B., Dumont, M.E. and Mauk, A.G. (1998) Biochemistry 37, 6124–6131.

[8] Morar, A.S., Kakouras, D., Young, G.B., Boyd, J. and Pielak, G.J. (1999) J. Biol. Inorg. Chem. 4, 220–222.

[9] Boyd, J., Dobson, C.M., Morar, A.S., Williams, R.J.P. and Pielak, G.J. (1999) J. Am. Chem. Soc. 121, 9247–9248.

[10] Tjandra, N. and Bax, A. (1997) Science 278, 1111–1114.

[11] Pearson, J.G., Wang, J.F., Markley, J.L., Le, H.B. and Oldfield, E. (1995) J. Am. Chem. Soc. 117, 8823–8829.

[12] Tjandra, N. and Bax, A. (1997) J. Am. Chem. Soc. 119, 9576–9577.

[13] de Dios, A.C., Pearson, J.G. and Oldfield, E. (1993) Science 260, 1491–1496.

[14] Le, H. and Oldfield, E. (1994) J. Biomol. NMR 4, 341–348.

[15] Sambrook, J., Fritsche, E.F. and Maniatis, T. (1989) Molecular Cloning: A Laboratory Manual, 2nd edn., Cold Spring Harbor Laboratory, New York.

[16] Margoliash, E. and Frohwirt, N. (1959) Biochem. J. 71, 570–572.

[17] Jennings, P.A., Stone, M.J. and Wright, P.E. (1995) J. Biomol. NMR 6, 271–276.

[18] Muhandiram, D.R. and Kay, L.E. (1994) J. Magn. Res. Ser. B 103, 203–216.

[19] Yamazaki, T., Weontae, L., Arrowsmith, C.H., Muhandiram, D.R. and Kay, L.E. (1994) J. Am. Chem. Soc. 116, 11655–11666.

[20] Grzesiek, S. and Bax, A. (1992) J. Magn. Reson. 96, 432–440.

[21] Wittekind, M. and Mueller, L. (1993) J. Magn. Reson. B 101, 201–205.

[22] Wishart, D.S., Bigam, C.G., Yao, J., Abildgaard, F., Dyson, H.J., Oldfield, E., Markley, J.L. and Sykes, B.D. (1995) J. Biomol. NMR 6, 135–140.

[23] Kay, L.E., Keifer, P. and Saarinen, T. (1992) J. Am. Chem. Soc. 114, 10663–10665.

[24] Smallcombe, S.H., Patt, S.L. and Keifer, P.A. (1995) J. Magn. Reson. A 117, 295–303.

[25] Powers, R., Gronenborn, A.M., Clore, G.M. and Bax, A. (1991) J. Magn. Reson. 94, 209–213.

[26] Sattler, M., Schwendinger, M.G., Schleucher, J. and Griesinger, C. (1995) J. Biomol. NMR 5, 11–22.

[27] Wang, A.C., Lodi, P.J., Qin, J., Vuister, G.W., Gronenborn, A.M. and Clore, G.M. (1994) J. Magn. Reson. B 105, 196–198.

[28] London, F. (1937) J. Phys. Radium 8, 397–409.

[29] Ditchfield, R. (1972) J. Chem. Phys. 56, 5688–5691.

[30] Frisch, M.J., Trucks, G.W., Schlegel, H.B., Scuseria, G.E., Robb, M.A., Cheeseman, J.R., Zakrzewski, V.G., Montgomery, J.A., Jr., Stratmann, R.E., Burant, J.C., Dapprich, S., Millam, J.M., Daniels, A.D., Kudin, K.N., Strain, M.C., Farkas, O., Tomasi, J., Barone, V., Cossi, M., Cammi, R., Mennucci, B., Pomelli, C., Adamo, C., Clifford, S., Ochterski, J., Petersson, G.A., Ayala, P.Y., Cui, Q., Morokuma, K., Malick, D.K., Rabuck, A.D., Raghavachari, K., Foresman, J.B., Cioslowski, J., Ortiz, J.V., Baboul, A.G., Stefanov, B.B., Liu, G., Liashenko, A., Piskorz, P., Komaromi, I., Gomperts, R., Martin, R.L., Fox, D.J., Keith, T., Al-Laham, M.A., Peng, C.Y., Nanayakkara, A., Gonzalez, C., Challacombe, M., Gill, P.M.W., Johnson, B., Chen, W., Wong, M.W., Andres, J.L., Gonzalez, C., Head-Gordon, M., Replogle, E.S. and Pople, J.A. (1998) Gaussian 98, Revision A.7, Gaussian, Inc., Pittsburgh, PA.

[31] Weiner, S.J., Kollman, P.A., Case, D.A., Singh, U.C., Ghio, C., Alagona, G., Profeta Jr., S. and Weiner, P. (1984) J. Am. Chem. Soc. 106, 765–784.

[32] Weiner, S.J., Kollman, P.A., Nguyen, D.T. and Case, D.A. (1986) J. Comp. Chem. 7, 230–252.

[33] Pearson, J.G., Le, H., Sanders, L.K., Godbout, N., Havlin, R.H. and Oldfield, E. (1997) J. Am. Chem. Soc. 119, 11941–11950.

[34] Chestnut, D.B. and Moore, K.D. (1989) J. Comput. Chem. 10, 648–659.

[35] Becke, A.D. (1988) Phys. Rev. A 38, 3098–3100.

[36] Perdew, J.P. and Wang, Y. (1992) Phys. Rev. B 45, 13244–13249.

[37] Berman, H.M., Westbrook, J., Feng, Z., Gilliland, G., Bhat, T.N., Weissig, H., Shindylalov, I.N. and Bourne, P.E. (2000) Nucleic Acids Res. 28, 235–242.

[38] Wlodawer, A., Walter, J., Huber, R. and Sjolin, L. (1984) J. Mol. Biol. 180, 301–329.

[39] Vijay-Kumar, S., Bugg, C.E. and Cook, W.J. (1987) J. Mol. Biol. 194, 531–544.

[40] Lo, T.P., Guillemette, J.G., Louie, G.V., Smith, M. and Brayer, G.D. (1995) Biochemistry 34, 163–171.

[41] Laws, D.D., de Dios, A.C. and Oldfield, E. (1993) J. Biomol. NMR 3, 607–612.

[42] Heller, J., Laws, D.D., Tomaselli, M., King, D.S., Wemmer, D.E., Pines, A., Havlin, R.H. and Oldfield, E. (1997) J. Am. Chem. Soc. 119, 7827–7831.

[43] Glushka, J., Lee, M., Coffin, S. and Cowburn, D. (1989) J. Am. Chem. Soc. 111, 7716–7722.

[44] Wang, A.C., Grzesiek, S., Tschudin, R., Lodi, P.J. and Bax, A. (1995) J. Biomol. NMR 5, 376–382.

[45] Cornilescu, G., Marquardt, J.L., Ottiger, M. and Bax, A. (1998) J. Am. Chem. Soc. 120, 6836.

[46] Berndt, K.D., Guntert, P., Orbons, L.P. and Wuthrich, K. (1992) J. Mol. Biol. 227, 757.